Acta Cryst E CRYSTALLOGRAPHIC COMMUNICATIONS

ISSN 2056-9890

# Crystal structure, Hirshfeld surface, DFT and molecular docking studies of 2-{4-[(*E*)-(4-acetylphenyl)diazenyl]phenyl}-1-(5-bromothiophen-2-yl)-ethanone; a compound with bromine···oxygen-type contacts

Received 25 September 2024
Accepted 7 November 2024

Edited by F. F. Ferreira, Universidade Federal do ABC, Brazil

**Keywords:** crystal structure; azobenzene; molecular docking; C—Br···O═C contact; DFT and Hirshfeld surface.

**CCDC reference:** 2401081

**Supporting information:** this article has supporting information at journals.iucr.org/e

S. Santhosh Kumar,[a] H.T Srinivasa,[b] M. Harish Kumar,[c] H. C. Devarajegowda[c] and B. S. Palakshamurthy[a]*

[a]Department of PG Studies and Research in Physics, Albert Einstein Block, UCS, Tumkur University, Tumkur, Karnataka-572103, India, [b]Raman Research Institute, C. V. Raman Avenue, Sadashivanagar, Bangalore, Karnataka, India, and [c]Department of Physics, Yuvaraja's College, University of Mysore, Mysore 570005, Karnataka, India. *Correspondence e-mail: palaksha.bspm@gmail.com

The title compound, $C_{19}H_{13}BrN_2O_3S$, a non-liquid crystal molecule, crystallizes in the orthorhombic system, space group $Pna2_1$. The torsion angles associated with ester and azo groups are −177.0 (4)°, -anti-periplanar, and 179.0 (4)°, +anti-periplanar, respectively. The packing is consolidated by a weak C—Br···O═C contact, forming infinite chains running along the [001] direction. A Hirshfeld surface analysis revealed that the major contributions to the crystal surface are from H···H, C···H/H···C, O···H/H···O, Br···H/H···Br and S···H/H···S interactions. The computed three-dimensional energy interactions using the basis set B3LYP\631-G(d,p) show that $E_{dis}$ (217.6 kJ mol$^{-1}$) is the major component in the structure. The DFT calculations performed at the B3LYP/6–311+ G(d,p) level indicate that the energy gap between HOMO and LUMO is 3.6725 (2) eV. The molecular electrostatic potential (MEP) map generated supports the existence of the Br···O type contact, formed between the electrophilic site of the bromine atom and the nucleophilic site of the ketonic oxygen atom. The molecular docking between the ligand and the *Mycobacterium Tuberculosis* (PDB ID:1HZP) receptor shows a good binding affinity value of −8.5 kcal mol$^{-1}$.

## 1. Chemical context

Azobenzenes are a class of molecules having high structural similarity with stilbenes, which exhibit antibacterial and antifungal activity (Piotto *et al.*, 2013). They are capable of regulating the structure and function of various biological molecules, including proteins, nucleic acids, lipids and peptides (Mulatihan *et al.*, 2020). Azobenzene derivatives exhibit biological activities such as antioxidant, antiviral and antimicrobial properties (Ventura & Wiedman, 2021; Kaur & Narasimhan, 2018; Peddie & Abell, 2019). Azobenzene-based polymeric nanocarriers are biocompatible materials and they can accelerate drug-release systems in biological tissues (Londoño-Berrío *et al.*, 2022). Interestingly thiophene-based derivatives exhibit significant anti-leishmanial activity (Félix *et al.*, 2016) and antimalarial activity (Akolkar *et al.*, 2022). The thiophene derivatives with antitubulin properties are potential materials for the treatment of cancer and Alzheimer's and Parkinson's diseases (Romagnoli *et al.*, 2007). The thiophene-thiazole derivatives are a class of materials having antitubulin properties and they can also be used as anti-breast cancer agents (Al-Said *et al.*, 2011). Azobenzenes, and their deriva-

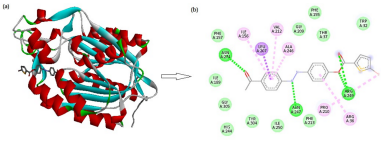

tives in a *trans* confirmation, are medically important. They are also useful in industry because of their interesting photoswitch properties and have therefore been widely explored as photoresponsive compounds in materials science (Li *et al.*, 2024). Keeping photoswitching properties in mind, we have planed to use the tris(azobenzene) as a core group in the construction of liquid-crystal materials. Hence, we developed the title molecule, (I), to analyse the molecular properties both experimentally and theoretically and present the results herein.

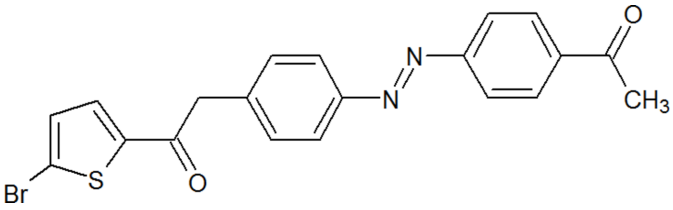


## 2. Structural commentary

The molecular structure of compound (I) is shown in Fig. 1. In the molecule, the dihedral angles between the five-membered thiophene and the benzene and phenylethanone rings are 1.6 (2) and 54.0 (2)°, respectively, while that between the aromatic rings is 52.5 (2)°. The torsion angles associated with the ester (C—C—O—C) and azo (C—N═N—C) groups in the molecule are -anti-periplanar [−177.0 (4)°] and +anti-periplanar [179.0 (4)°], respectively. Intramolecular C13—H13···N1, C10—H10···N2, and C16—H16···O3 interactions (Table 1) stabilize the molecular structure.

## 3. Supramolecular features

The crystal packing is consolidated by C1—Br1···O3═C18 type interaction with a Br1···O3 distance 3.014 (2) Å, forming infinite chains running in the [001] direction as shown in Fig. 2.

## 4. Database survey

A search of the Cambridge Structural Database (CSD, version 5.42, update of November 2020; Groom *et al.*, 2016) for molecules containing the *trans*(azobenzene) fragment resulted in two matches with CSD refcodes APOPUR, APOQAY and APOQEC (Soegiarto *et al.*, 2010). In APOPUR, 4,4′-azobenzenedisulfonate is associated with two azobenzene molecules, one of which is disordered, with the another having a tris conformation. The torsion angles at the azo and azobenzene groups are180.00 and −179.96°. In APOQAY, the 4,4′- dibenzyldisulfonate moiety is associated with two azobenzene fragments in which the torsion angles at the azo groups are 180.0 and178.39° and have a tris conformation. In APOQEC, the 4,4′-stilbenedisulfonate is associated with two azobenzene moieties with torsion angles at the azo group of 180 and −177.93 (2)°. These are comparable with the torsion angle at the azo group of 179.0 (4)° in the tris(azobenzene) fragment of the title molecule. In all these compounds, the torsion angles at the azo group are *anti.*.

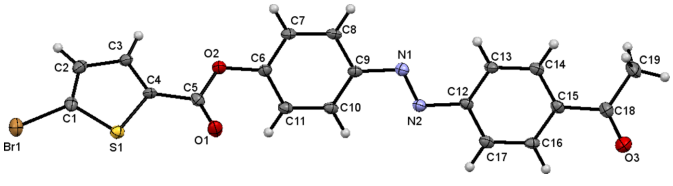


**Figure 1**
Molecular structure of the title compound, showing displacement ellipsoids drawn at the 50% probability level.

**Table 1**
Hydrogen-bond geometry (Å, °).

| *D*—H···*A* | *D*—H | H···*A* | *D*···*A* | *D*—H···*A* |
|---|---|---|---|---|
| C13—H13···N1 | 0.95 | 2.47 | 2.722 (6) | 95 |
| C16—H16···O3 | 0.95 | 2.49 | 2.788 (6) | 98 |
| C10—H10···N2 | 0.95 | 2.45 | 2.705 (6) | 95 |

## 5. Hirshfeld surface analysis and interaction energies

A Hirshfeld surface analysis was carried out to quantify the various intermolecular interactions contributed to the crystal using *CrystalExplorer17.5* (Turner *et al.*, 2017). Fig. 3 illustrates the Hirshfeld surface mapped over $d_{norm}$ with red spots corresponding to short C—Br···O═C contacts. It is an additional confirmation of the presence of Br···O type contacts (*i.e* halogen–oxygen type). In Fig. 4, the sharp spikes in the Br···O/O···Br fingerprint plot indicate the existence of a weak halogen···oxygen interaction in the molecular structure. Although it is a weak interaction, the packing of the title compound is consolidated by Br···O interactions and no

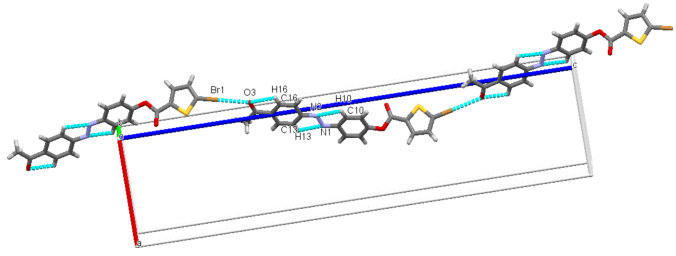


**Figure 2**
Molecular packing of the title compound, Dashed lines indicate C—Br···O═C intramolecular contacts.

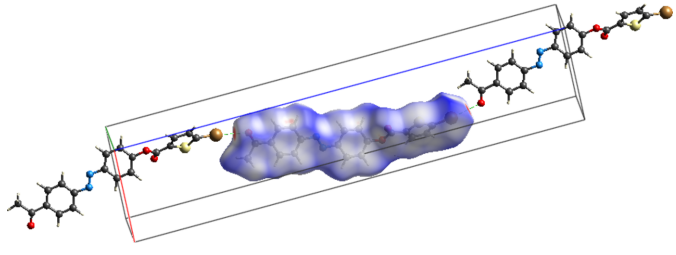

**Figure 3**
Hirshfeld surface mapped over $d_{norm}$ with red spots corresponding to short C—Br···O═C contacts.

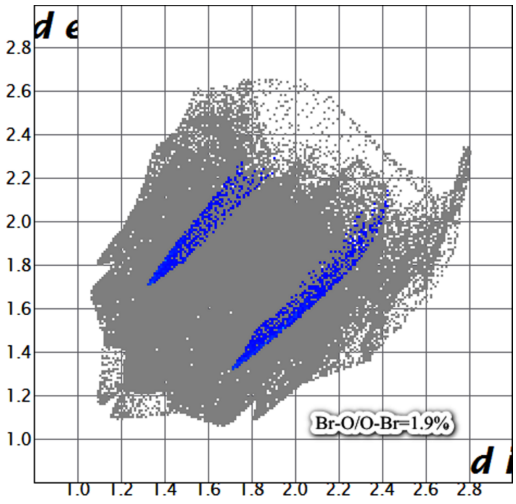


**Figure 4**
The two-dimensional fingerprint plots (spikes) showing the halogen–oxygen interactions.

other interactions are present. The fingerprint plots showing all interactions and those delineated into H···H, C···H/H···C, O···H/ H···O, Br···H/H···Br and S···H/H···S interactions as shown in Fig. 5.

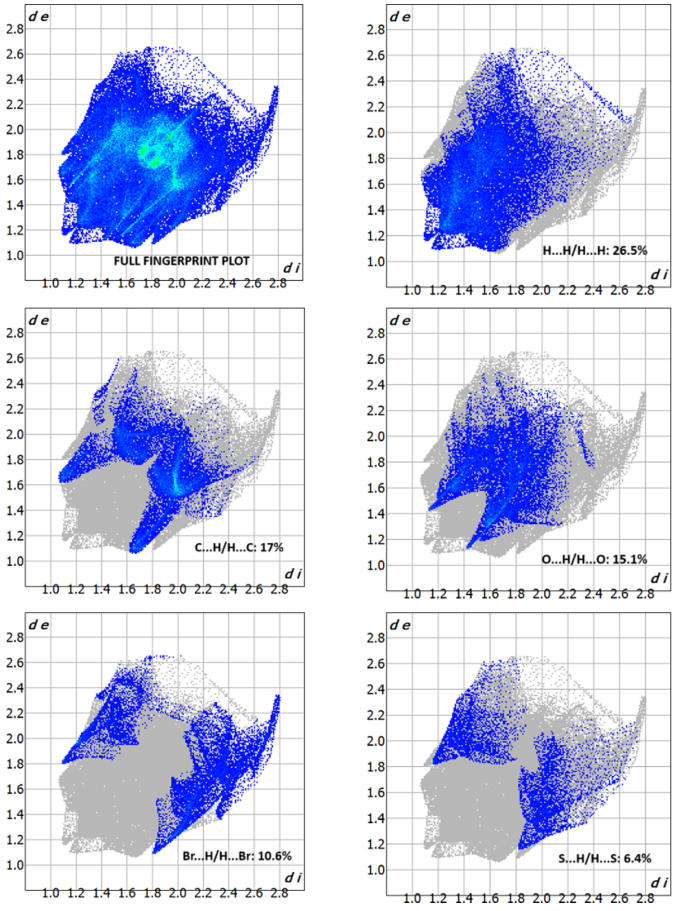


**Figure 5**
The two-dimensional fingerprint plots showing all interactions and those delineated into H···H, C···H/H···C, O···H/ H···O, Br···H/H···Br and S···H/H···S interactions.

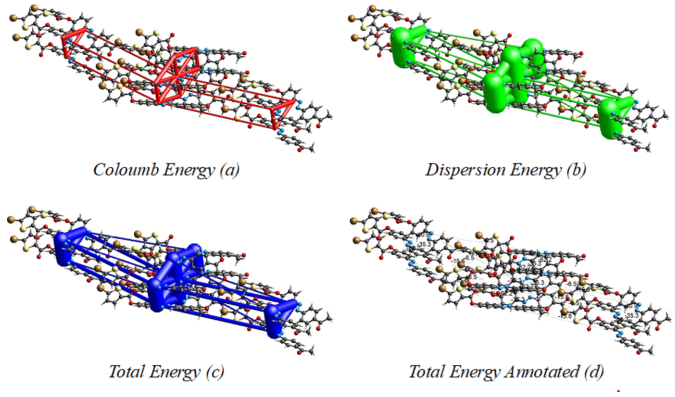


**Figure 6**
The energy frameworks for the interaction energies in the title compound (*a*) Coulombic energy, (*b*) dispersion energy, (*c*) total energy and (*d*) total energy annotated.

Three-dimensional energy interactions were computed for the title compound using the B3LYP\631-G(d,p) basis set, indicating that the $E_{dis}$ = 217.6 kJ mol$^{-1}$ is the major component, the others being $E_{ele}$ = 55.3 kJ mol$^{-1}$, $E_{pol}$ =11.6 kJ mol$^{-1}$, $E_{rep}$ = 148.6 kJ mol$^{-1}$ with a total interaction energy $E_{tot}$ of 164.7 kJ mol$^{-1}$. The energy frameworks for the interaction energies are shown in Fig. 6.

## 6. DFT Studies

The molecular structure of the title compound in the gas phase was optimized using density functional theory with the standard B3LYP method with the basis set 6-311++G(d,p). The input files were prepared from the CIF file using *Mercury* (Macrae *et al.*, 2020) and *Gauss View* 6.0 (Frisch *et al.*, 2009). The electron density distribution in the frontier molecular orbital are shown in Fig. 7. The highest occupied molecular orbital (HOMO) is −6.7179 eV) and the lowest unoccupied molecular orbital (LUMO) is −3.0454 eV) with an energy gap of 3.6725 eV. The electrophilicity index ($\omega$) is 6.489 eV, which indicates the molecule is highly reactive.

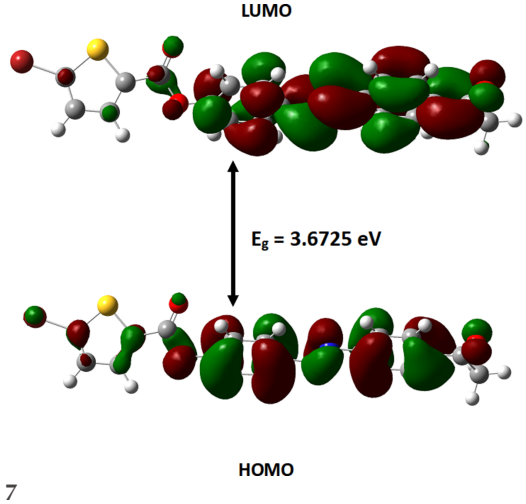


**Figure 7**
The HOMO and LUMO orbitals of the title molecule.

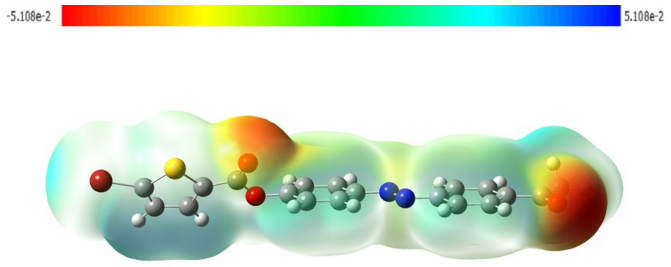


**Figure 8**
The molecular electrostatic potential (MEP) surface of the title molecule.

The molecular electrostatic potential (MEP) map predicts the reactive sites for electrophilic and nucleophilic attack present in the molecule. In the crystal, the molecular charge distribution is between $-5.108 \times 10^{-2}$ and $+5.108 \times 10^{-2}$ and is governed by the MEP (Fig. 8). The red colour around the oxygen atoms of the ester group and ketone group in the molecule indicates nucleophilic sites and the pale-blue colour around the bromine atom indicate the active electrophilic site. In the crystal, the Br···O type contact formed between the electrophilic site of the bromine atom and the nucleophilic site of the ketonic oxygen atom connects the molecule into infinite chains along the *c*-axis direction.

## 7. Molecular docking

The molecular docking studies using *AutoDock* tools (Huey *et al.*, 2012) were carried out to calculate the degree of binding affinity between the synthesised ligand and the receptor protein of *Mycobacterium Tuberculosis* bacteria (PDB ID:1HZP). It is found that, among the several interactions with the target protein, four conventional hydrogen-bonding interactions are seen between four moieties, which are formed by the oxygen and nitrogen atoms of the ketonic, ester and azo groups, as shown in Fig. 9. The centroids of the benzene rings (*Cg*1, C6–C11 and *Cg*2, C12–C17) attack different amino acid groups (ILE A:156, VAL A:212, ALA A:246 and ARG A:36). *PLATON* (Spek, 2020) indicates very weak $\pi$–$\pi$ stacking between these rings with *Cg*1···*Cg*2 separations of 5.609 (3) to 5.616 (2) Å; these stacking interactions were able to attack the aforementioned amino acids of the protein. In addition to these, the bromine atom in the molecule has an affinity with another amino acid group (PRO A:210) through nucleophilic attacks. In total, the ligand shows a good binding affinity value of $-8.5$ kcal mol$^{-1}$.

## 8. Synthesis and crystallization

5-Bromothiophene-2-carboxylic acid (1 eq, 0.207 g), (*E*)-1-{4-[(4-hydroxyphenyl)diazenyl]phenyl}ethan-1-one (1 eq, 0.240 g), dicyclohexylcarbodiimide (1.2 eq) and a catalytic amount of dimethylaminopyrimidine were stirred in dry dichloromethane at room temperature overnight. Completion of the reaction was verified by thin layer chromatography on silica gel on an aluminium plate with dichloromethane as the mobile phase. After completion of the reaction, the whole reaction mass was subjected to column chromatography with silica gel and a 1:9 ratio of petroleum ether and dichloromethane as eluent. The solvent was evaporated under vacuum, and the crude product was recrystallized from pure chloroform to obtain single crystals suitable for single-crystal X-ray studies. The compound is orange in colour, m.p. 469 K, molecular weight is 429.29. Elemental analysis, calculated: C, 53.16; H, 3.05; Br, 18.61; N, 6.53; O, 11.18; S, 7.47; found: C, 53.19; H, 3.09; N, 6.60; S, 7.52%. $^1$H NMR: (500 MHz, $CDCl_3$) $\delta$/ppm, 8.13–7.97 (*m*, 6H, Ar-H), 7.76 (*d*, 1H, $J$ = 6 Hz, Ar-H), 7.43 (*m*, 2H, Ar-H), 7.18 (*m*, 1H, Ar-H), 1.57 (*s*, 3H, $COCH_3$) ppm. $^{13}$C NMR ($CDCl_3$) $\delta$/ppm: 197.5, 159.1, 154.9, 152.8, 138.5, 135.3, 131.4, 122.9, 26.9.

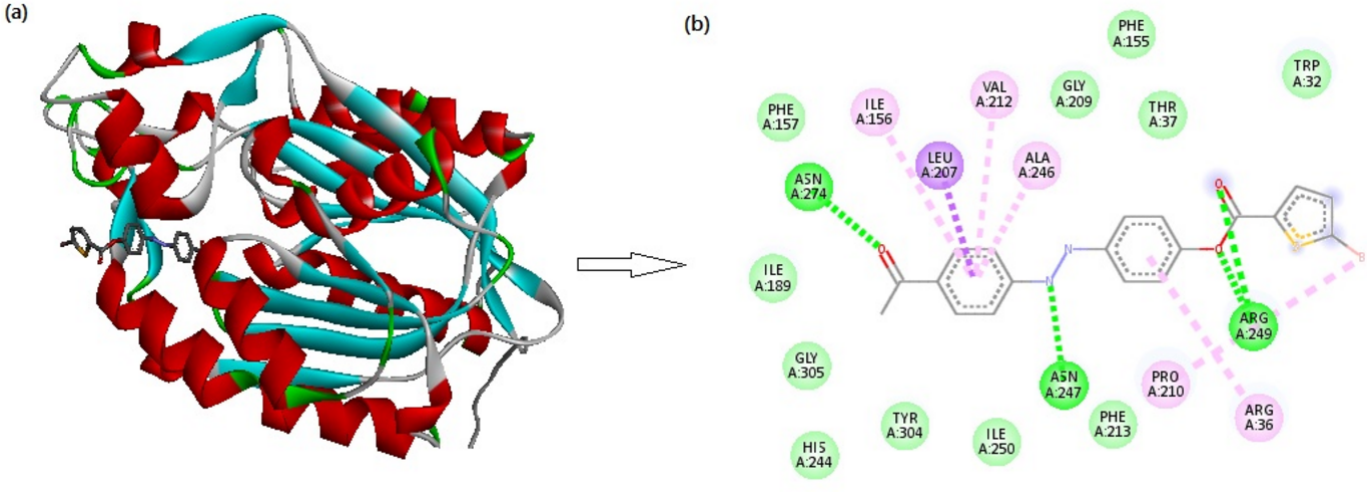


**Figure 9**
Three-dimensional and two-dimensional views of various interactions between the title compound (ligand) and *Myobacterium Tuberculosis* bacteria (PDB ID:1HZP; receptor protein).

## 9. Refinement

Crystal data, data collection and structure refinement details are summarized in Table 2. All the H-atoms were positioned with idealized geometry and refined using a riding model with C—H = 0.95–0.98 Å and $U_{iso}$(H) = 1.2$U_{eq}$(C) or 1.5$U_{eq}$(methyl C). The crystal studied was refined as an inversion twin.


## Acknowledgements

The authors thank Kishore and Shivakumar, C., SSCU, IISc, for their help in collecting the SCXRD data and the BSPM lab, Albert Einstein Block, UCS, for the software and other facilities to complete this work.

## Funding information

Funding for this research was provided by: Vision Group of Science and Technology (award No. GRD319 to B. S. Palakshamurthy).


**Table 2**
Experimental details.

| | |
|---|---|
| Crystal data | |
| Chemical formula | $C_{19}H_{13}BrN_2O_3S$ |
| $M_r$ | 429.28 |
| Crystal system, space group | Orthorhombic, $Pna2_1$ |
| Temperature (K) | 120 |
| $a$, $b$, $c$ (Å) | 10.5425 (13), 3.8532 (5), 42.419 (4) |
| $V$ (Å$^3$) | 1723.1 (4) |
| $Z$ | 4 |
| Radiation type | Mo $K\alpha$ |
| $\mu$ (mm$^{-1}$) | 2.53 |
| Crystal size (mm) | 0.41 × 0.28 × 0.18 |
| | |
| Data collection | |
| Diffractometer | Bruker *SMART* APEXII CCD |
| Absorption correction | Multi-scan (*SADABS*; Krause *et al.*, 2015) |
| $T_{min}$, $T_{max}$ | 0.431, 0.633 |
| No. of measured, independent and observed [$I > 2\sigma(I)$] reflections | 36482, 5305, 5216 |
| $R_{int}$ | 0.029 |
| (sin $\theta/\lambda)_{max}$ (Å$^{-1}$) | 0.716 |
| | |
| Refinement | |
| $R[F^2 > 2\sigma(F^2)]$, $wR(F^2)$, $S$ | 0.037, 0.091, 1.23 |
| No. of reflections | 5305 |
| No. of parameters | 237 |
| No. of restraints | 1 |
| H-atom treatment | H-atom parameters constrained |
| $\Delta\rho_{max}$, $\Delta\rho_{min}$ (e Å$^{-3}$) | 1.12, −1.54 |
| Absolute structure | Refined as an inversion twin |
| Absolute structure parameter | 0.021 (12) |

Computer programs: *APEX2* and *SAINT* (Bruker, 2014), *SHELXS97* (Sheldrick, 2008), *SHELXL2018/3* (Sheldrick, 2015) and *Mercury* (Macrae *et al.*, 2020).

## References


Akolkar, H. N., Dengale, S. G., Deshmukh, K. K., Karale, B. K., Darekar, N. R., Khedkar, V. M. & Shaikh, M. H. (2022). *Polycyclic Aromat. Compd.* **42**, 1959–1971.

Al-Said, M. S., Bashandy, M. S., Al-qasoumi, S. I. & Ghorab, M. M. (2011). *Eur. J. Med. Chem.* **46**, 137–141.

Bruker (2014). *APEX2* and *SAINT*. Bruker AXS Inc., Madison, Wisconsin, USA.

Félix, M. B., de Souza, E. R., de Lima, M. D. C., Frade, D. K. G., Serafim, V. L., Rodrigues, K. A. D. F., Néris, P. L. D. N., Ribeiro, F. F., Scotti, L., Scotti, M. T., de Aquino, T. M., Mendonça Junior, F. J. B. & de Oliveira, M. R. (2016). *Bioorg. Med. Chem.* **24**, 3972–3977.

Frisch, M. J., Trucks, G. W., Schlegel, H. B., Scuseria, G. E., Robb, M. A., Cheeseman, J. R., Scalmani, G., Barone, V., Mennucci, B., Petersson, G. A., Nakatsuji, H., Caricato, M., Li, X., Hratchian, H. P., Izmaylov, A. F., Bloino, J., Zheng, G., Sonnenberg, J. L., Hada, M., Ehara, M., Toyota, K., Fukuda, R., Hasegawa, J., Ishida, M., Nakajima, T., Honda, Y., Kitao, O., Nakai, H., Vreven, T., Montgomery, J. A. Jr, Peralta, J. E., Ogliaro, F., Bearpark, M., Heyd, J. J., Brothers, E., Kudin, K. N., Staroverov, V. N., Kobayashi, R., Normand, J., Raghavachari, K., Rendell, A., Burant, J. C., Iyengar, S. S., Tomasi, J., Cossi, M., Rega, N., Millam, J. M., Klene, M., Knox, J. E., Cross, J. B., Bakken, V., Adamo, C., Jaramillo, J., Gomperts, R., Stratmann, R. E., Yazyev, O., Austin, A. J., Cammi, R., Pomelli, C., Ochterski, J. W., Martin, R. L., Morokuma, K., Zakrzewski, V. G., Voth, G. A., Salvador, P., Dannenberg, J. J., Dapprich, S., Daniels, A. D., Farkas, O., Foresman, J. B., Ortiz, J. V., Cioslowski, J. & Fox, D. J. (2009). *Gaussian 09W*, Revision A. 02, Gaussian, Inc., Wallingford CT, USA.

Groom, C. R., Bruno, I. J., Lightfoot, M. P. & Ward, S. C. (2016). *Acta Cryst.* B**72**, 171–179.

Huey, R., Morris, G. M. & Forli, S. (2012). *AutoDock*. The Scripps Research Institute Molecular Graphics Laboratory, La Jolla, California, USA.

Kaur, H. & Narasimhan, B. (2018). *Curr. Top. Med. Chem.* **18**, 3–21.

Krause, L., Herbst-Irmer, R., Sheldrick, G. M. & Stalke, D. (2015). *J. Appl. Cryst.* **48**, 3–10.

Li, Y., Xue, B., Yang, J., Jiang, J., Liu, J., Zhou, Y., Zhang, J., Wu, M., Yuan, Y., Zhu, Z., Wang, Z. J., Chen, Y., Harabuchi, Y., Nakajima, T., Wang, W., Maeda, S., Gong, J. P. & Cao, Y. (2024). *Nat. Chem.* **16**, 446–455.

Londoño-Berrío, M., Pérez-Buitrago, S., Ortiz-Trujillo, I. C., Hoyos-Palacio, L. M., Orozco, L. Y., López, L., Zárate-Triviño, D. G., Capobianco, J. A. & Mena-Giraldo, P. (2022). *Polymers*, **14**, 3119.

Macrae, C. F., Sovago, I., Cottrell, S. J., Galek, P. T. A., McCabe, P., Pidcock, E., Platings, M., Shields, G. P., Stevens, J. S., Towler, M. & Wood, P. A. (2020). *J. Appl. Cryst.* **53**, 226–235.

Mulatihan, D., Guo, T. & Zhao, Y. (2020). *Photochem. & Photobiol.* **96**, 1163–1168.

Peddie, V. & Abell, A. D. J. (2019). *J. Photochem. Photobiol. Photochem. Rev.* **40**, 1–20.

Piotto, S., Concilio, S., Sessa, L., Porta, A., Calabrese, E. C., Zanfardino, A., Varcamonti, M. & Iannelli, P. (2013). *Eur. J. Med. Chem.* **68**, 178–184.

Romagnoli, R., Baraldi, P. G., Carrion, M. D., Lopez Cara, C., Preti, D., Fruttarolo, F., Pavani, M. G., Tabrizi, M. A., Tolomeo, M., Grimaudo, S., Di Cristina, A., Balzarini, J., Hadfield, J. A., Brancale, A. & Hamel, E. (2007). *J. Med. Chem.* **50**, 2273–2277.

Sheldrick, G. M. (2008). *Acta Cryst.* A**64**, 112–122.

Sheldrick, G. M. (2015). *Acta Cryst.* C**71**, 3–8.

Soegiarto, A. C., Comotti, A. & Ward, M. D. (2010). *J. Am. Chem. Soc.* **132**, 14603–14616.

Spek, A. L. (2020). *Acta Cryst.* E**76**, 1–11.

Turner, M. J., MacKinnon, J. J., Wolff, S. K., Grimwood, D. J., Spackman, P. R., Jayatilaka, D. & Spackman, M. A. (2017). *CrystalExplorer17.5*. University of Western Australia. http:// hirshfeldsurface. net.

Ventura, C. R. & Wiedman, G. R. (2021). *Biochim. Biophys. Acta*, **1863**, 183759.

# supporting information

*Acta Cryst.* (2024). E**80**, 1308-1312 [https://doi.org/10.1107/S2056989024010776]

# Crystal structure, Hirshfeld surface, DFT and molecular docking studies of 2-{4-[(*E*)-(4-acetylphenyl)diazenyl]phenyl}-1-(5-bromothiophen-2-yl)ethanone; a compound with bromine···oxygen-type contacts

**S. Santhosh Kumar, H.T Srinivasa, M. Harish Kumar, H. C. Devarajegowda and B. S. Palakshamurthy**

## Computing details

### 2-{4-[(*E*)-(4-Acetylphenyl)diazenyl]phenyl}-1-(5-bromothiophen-2-yl)ethanone

*Crystal data*

$C_{19}H_{13}BrN_2O_3S$
$M_r$ = 429.28
Orthorhombic, $Pna2_1$
Hall symbol: P 2c -2n
$a$ = 10.5425 (13) Å
$b$ = 3.8532 (5) Å
$c$ = 42.419 (4) Å
$V$ = 1723.1 (4) Å$^3$
$Z$ = 4
$F(000)$ = 864
$D_x$ = 1.655 Mg m$^{-3}$
Melting point: 469 K
Mo $K\alpha$ radiation, $\lambda$ = 0.71074 Å
Cell parameters from 5305 reflections
$\theta$ = 2.8–30.1°
$\mu$ = 2.53 mm$^{-1}$
$T$ = 120 K
Prism, orange
0.41 × 0.28 × 0.18 mm

*Data collection*

Bruker SMART APEXII CCD diffractometer
Radiation source: fine-focus sealed tube
Graphite monochromator
Detector resolution: 0.99 pixels mm$^{-1}$
$\varphi$ and Ω scans
Absorption correction: multi-scan (SADABS; Krause *et al.*, 2015)
$T_{min}$ = 0.431, $T_{max}$ = 0.633
36482 measured reflections
5305 independent reflections
5216 reflections with $I > 2\sigma(I)$
$R_{int}$ = 0.029
$\theta_{max}$ = 30.6°, $\theta_{min}$ = 2.9°
$h$ = −15→15
$k$ = −5→5
$l$ = −60→60

*Refinement*

Refinement on $F^2$
Least-squares matrix: full
$R[F^2 > 2\sigma(F^2)]$ = 0.037
$wR(F^2)$ = 0.091
$S$ = 1.23
5305 reflections
237 parameters
1 restraint
0.132 constraints
Primary atom site location: structure-invariant direct methods
Secondary atom site location: difference Fourier map
Hydrogen site location: inferred from neighbouring sites
H-atom parameters constrained
$w = 1/[\sigma^2(F_o^2) + (0.0229P)^2 + 3.5453P]$ where $P = (F_o^2 + 2F_c^2)/3$
$(\Delta/\sigma)_{max} < 0.001$

$\Delta\rho_{max}$ = 1.12 e Å$^{-3}$
$\Delta\rho_{min}$ = −1.54 e Å$^{-3}$

Absolute structure: Refined as an inversion twin
Absolute structure parameter: 0.021 (12)

*Special details*

**Geometry**. All esds (except the esd in the dihedral angle between two l.s. planes) are estimated using the full covariance matrix. The cell esds are taken into account individually in the estimation of esds in distances, angles and torsion angles; correlations between esds in cell parameters are only used when they are defined by crystal symmetry. An approximate (isotropic) treatment of cell esds is used for estimating esds involving l.s. planes.

**Refinement**. Refined as a 2-component inversion twin

*Fractional atomic coordinates and isotropic or equivalent isotropic displacement parameters (Å$^2$)*

| | *x* | *y* | *z* | $U_{iso}$*/$U_{eq}$ |
|---|---|---|---|---|
| Br1 | 0.72359 (4) | 0.43138 (12) | 0.72407 (2) | 0.02567 (11) |
| S1 | 0.65138 (10) | 0.3319 (3) | 0.65409 (3) | 0.01799 (19) |
| O2 | 0.7849 (3) | 0.5368 (9) | 0.56998 (7) | 0.0209 (6) |
| O1 | 0.6053 (3) | 0.2541 (11) | 0.58516 (8) | 0.0261 (7) |
| O3 | 0.3469 (4) | 0.5729 (11) | 0.29358 (10) | 0.0296 (9) |
| C2 | 0.8653 (4) | 0.6201 (12) | 0.66779 (11) | 0.0213 (9) |
| H2 | 0.934208 | 0.714315 | 0.679421 | 0.026* |
| N1 | 0.6770 (4) | 0.4543 (10) | 0.44152 (9) | 0.0180 (7) |
| N2 | 0.5674 (3) | 0.5376 (10) | 0.43322 (9) | 0.0181 (7) |
| C3 | 0.8591 (4) | 0.6110 (12) | 0.63421 (10) | 0.0173 (8) |
| H3 | 0.924322 | 0.694646 | 0.620752 | 0.021* |
| C6 | 0.7507 (4) | 0.5120 (11) | 0.53813 (10) | 0.0167 (7) |
| C18 | 0.4512 (4) | 0.4762 (13) | 0.30191 (11) | 0.0213 (8) |
| C8 | 0.8114 (4) | 0.3473 (12) | 0.48602 (10) | 0.0177 (8) |
| H8 | 0.870799 | 0.246549 | 0.471880 | 0.021* |
| C17 | 0.4310 (4) | 0.6460 (12) | 0.38941 (10) | 0.0186 (8) |
| H17 | 0.372427 | 0.744592 | 0.403888 | 0.022* |
| C11 | 0.6381 (4) | 0.6597 (12) | 0.52722 (10) | 0.0184 (8) |
| H11 | 0.580744 | 0.768563 | 0.541366 | 0.022* |
| C13 | 0.6316 (4) | 0.3619 (12) | 0.37891 (10) | 0.0177 (8) |
| H13 | 0.709212 | 0.267351 | 0.386355 | 0.021* |
| C14 | 0.6021 (4) | 0.3488 (12) | 0.34710 (10) | 0.0178 (8) |
| H14 | 0.659950 | 0.245795 | 0.332706 | 0.021* |
| C16 | 0.4025 (4) | 0.6309 (11) | 0.35762 (11) | 0.0169 (8) |
| H16 | 0.323815 | 0.720403 | 0.350343 | 0.020* |
| C9 | 0.6980 (4) | 0.4834 (11) | 0.47477 (10) | 0.0161 (7) |
| C7 | 0.8372 (4) | 0.3598 (12) | 0.51804 (10) | 0.0181 (8) |
| H7 | 0.913759 | 0.264461 | 0.526070 | 0.022* |
| C1 | 0.7600 (4) | 0.4768 (12) | 0.68108 (10) | 0.0199 (8) |
| C4 | 0.7478 (4) | 0.4672 (12) | 0.62360 (10) | 0.0158 (7) |
| C12 | 0.5465 (4) | 0.5149 (11) | 0.39993 (10) | 0.0159 (7) |
| C10 | 0.6122 (4) | 0.6435 (11) | 0.49528 (10) | 0.0169 (7) |
| H10 | 0.535967 | 0.741241 | 0.487273 | 0.020* |
| C5 | 0.7016 (4) | 0.4050 (11) | 0.59146 (10) | 0.0182 (8) |
| C15 | 0.4873 (4) | 0.4867 (11) | 0.33604 (10) | 0.0175 (8) |
| C19 | 0.5478 (5) | 0.3457 (17) | 0.27848 (12) | 0.0320 (11) |

| | | | | |
|---|---|---|---|---|
| H19A | 0.578978 | 0.117756 | 0.285185 | 0.048* |
| H19B | 0.618949 | 0.509129 | 0.277391 | 0.048* |
| H19C | 0.508350 | 0.325653 | 0.257643 | 0.048* |

*Atomic displacement parameters (Å²)*

| | $U^{11}$ | $U^{22}$ | $U^{33}$ | $U^{12}$ | $U^{13}$ | $U^{23}$ |
|---|---|---|---|---|---|---|
| Br1 | 0.0321 (2) | 0.02593 (19) | 0.01893 (16) | −0.00111 (18) | −0.0019 (2) | 0.0010 (2) |
| S1 | 0.0169 (4) | 0.0172 (4) | 0.0199 (4) | −0.0016 (4) | 0.0006 (4) | −0.0011 (4) |
| O2 | 0.0166 (14) | 0.0271 (16) | 0.0189 (14) | −0.0018 (13) | 0.0006 (11) | −0.0014 (12) |
| O1 | 0.0262 (17) | 0.0306 (19) | 0.0214 (15) | −0.0109 (15) | 0.0015 (13) | −0.0022 (15) |
| O3 | 0.0244 (17) | 0.038 (2) | 0.0266 (18) | 0.0038 (16) | −0.0022 (15) | −0.0007 (16) |
| C2 | 0.0172 (19) | 0.022 (2) | 0.025 (2) | 0.0016 (16) | −0.0047 (15) | −0.0030 (16) |
| N1 | 0.0166 (15) | 0.0185 (16) | 0.0189 (16) | 0.0009 (13) | 0.0018 (13) | 0.0005 (14) |
| N2 | 0.0151 (15) | 0.0209 (17) | 0.0183 (16) | −0.0007 (14) | 0.0023 (13) | −0.0016 (13) |
| C3 | 0.0128 (17) | 0.020 (2) | 0.0193 (18) | −0.0001 (15) | −0.0004 (14) | 0.0010 (15) |
| C6 | 0.0141 (17) | 0.0180 (18) | 0.0179 (17) | −0.0029 (14) | 0.0008 (14) | −0.0004 (15) |
| C18 | 0.024 (2) | 0.022 (2) | 0.0188 (19) | 0.0004 (17) | 0.0018 (16) | −0.0020 (16) |
| C8 | 0.0114 (16) | 0.0192 (19) | 0.0225 (19) | −0.0002 (15) | 0.0046 (14) | −0.0009 (15) |
| C17 | 0.0166 (18) | 0.0174 (18) | 0.0217 (19) | −0.0016 (16) | 0.0043 (15) | −0.0015 (15) |
| C11 | 0.0156 (18) | 0.0177 (18) | 0.0218 (18) | 0.0006 (15) | 0.0028 (14) | −0.0037 (15) |
| C13 | 0.0134 (16) | 0.0199 (19) | 0.0198 (18) | 0.0023 (15) | 0.0028 (14) | −0.0001 (15) |
| C14 | 0.0162 (17) | 0.0159 (18) | 0.0213 (18) | −0.0012 (15) | 0.0042 (15) | −0.0019 (15) |
| C16 | 0.0135 (17) | 0.0138 (18) | 0.0234 (19) | 0.0011 (14) | 0.0019 (15) | −0.0024 (16) |
| C9 | 0.0132 (16) | 0.0148 (18) | 0.0202 (17) | −0.0013 (14) | 0.0021 (13) | 0.0006 (14) |
| C7 | 0.0127 (17) | 0.0193 (18) | 0.0222 (19) | 0.0027 (15) | 0.0018 (15) | −0.0009 (15) |
| C1 | 0.023 (2) | 0.0185 (19) | 0.0181 (18) | 0.0058 (16) | −0.0019 (15) | −0.0024 (15) |
| C4 | 0.0105 (16) | 0.0177 (18) | 0.0193 (18) | −0.0005 (14) | 0.0010 (13) | −0.0002 (14) |
| C12 | 0.0141 (17) | 0.0149 (17) | 0.0186 (17) | −0.0022 (14) | 0.0029 (14) | −0.0008 (14) |
| C10 | 0.0142 (17) | 0.0151 (17) | 0.0214 (19) | −0.0015 (15) | 0.0026 (14) | −0.0018 (15) |
| C5 | 0.0205 (19) | 0.0163 (19) | 0.0179 (17) | 0.0006 (15) | 0.0033 (15) | −0.0023 (15) |
| C15 | 0.0183 (18) | 0.0163 (18) | 0.0179 (18) | −0.0032 (15) | 0.0034 (14) | 0.0009 (15) |
| C19 | 0.033 (3) | 0.041 (3) | 0.022 (2) | 0.009 (2) | 0.0062 (19) | −0.005 (2) |

*Geometric parameters (Å, º)*

| | | | |
|---|---|---|---|
| Br1—C1 | 1.872 (4) | C8—C7 | 1.386 (6) |
| S1—C1 | 1.713 (5) | C8—C9 | 1.391 (6) |
| S1—C4 | 1.725 (4) | C8—H8 | 0.9500 |
| O2—C5 | 1.364 (5) | C17—C16 | 1.383 (6) |
| O2—C6 | 1.402 (5) | C17—C12 | 1.392 (6) |
| O1—C5 | 1.200 (6) | C17—H17 | 0.9500 |
| O3—O3 | 0.000 (15) | C11—C10 | 1.384 (6) |
| O3—C18 | 1.214 (6) | C11—H11 | 0.9500 |
| C2—C1 | 1.362 (7) | C13—C14 | 1.385 (6) |
| C2—C3 | 1.427 (6) | C13—C12 | 1.396 (6) |
| C2—H2 | 0.9500 | C13—H13 | 0.9500 |
| N1—N1 | 0.000 (13) | C14—C15 | 1.403 (6) |

| | | | |
|---|---|---|---|
| N1—N2 | 1.250 (5) | C14—H14 | 0.9500 |
| N1—N2 | 1.250 (5) | C16—C15 | 1.394 (6) |
| N1—C9 | 1.432 (6) | C16—H16 | 0.9500 |
| N2—N2 | 0.000 (13) | C9—C10 | 1.398 (6) |
| N2—C12 | 1.432 (5) | C7—H7 | 0.9500 |
| C3—C4 | 1.374 (6) | C4—C5 | 1.467 (6) |
| C3—H3 | 0.9500 | C10—H10 | 0.9500 |
| C6—C7 | 1.379 (6) | C19—H19A | 0.9800 |
| C6—C11 | 1.395 (6) | C19—H19B | 0.9800 |
| C18—C15 | 1.497 (6) | C19—H19C | 0.9800 |
| C18—C19 | 1.510 (6) | | |

| | | | |
|---|---|---|---|
| C1—S1—C4 | 90.5 (2) | C17—C16—H16 | 119.4 |
| C5—O2—C6 | 116.9 (3) | C15—C16—H16 | 119.4 |
| C1—C2—C3 | 111.5 (4) | C8—C9—C10 | 120.6 (4) |
| C1—C2—H2 | 124.3 | C8—C9—N1 | 116.2 (4) |
| C3—C2—H2 | 124.3 | C10—C9—N1 | 123.2 (4) |
| N2—N1—C9 | 113.6 (4) | C8—C9—N1 | 116.2 (4) |
| N2—N1—C9 | 113.6 (4) | C10—C9—N1 | 123.2 (4) |
| N1—N2—C12 | 113.9 (3) | C6—C7—C8 | 119.4 (4) |
| N1—N2—C12 | 113.9 (3) | C6—C7—H7 | 120.3 |
| C4—C3—C2 | 112.1 (4) | C8—C7—H7 | 120.3 |
| C4—C3—H3 | 123.9 | C2—C1—S1 | 113.6 (3) |
| C2—C3—H3 | 123.9 | C2—C1—Br1 | 127.5 (3) |
| C7—C6—C11 | 122.1 (4) | S1—C1—Br1 | 118.9 (3) |
| C7—C6—O2 | 117.0 (4) | C3—C4—C5 | 130.8 (4) |
| C11—C6—O2 | 120.7 (4) | C3—C4—S1 | 112.3 (3) |
| O3—C18—C15 | 120.2 (4) | C5—C4—S1 | 116.8 (3) |
| O3—C18—C15 | 120.2 (4) | C17—C12—C13 | 120.7 (4) |
| O3—C18—C19 | 121.5 (5) | C17—C12—N2 | 115.4 (4) |
| O3—C18—C19 | 121.5 (5) | C13—C12—N2 | 123.8 (4) |
| C15—C18—C19 | 118.3 (4) | C17—C12—N2 | 115.4 (4) |
| C7—C8—C9 | 119.5 (4) | C13—C12—N2 | 123.8 (4) |
| C7—C8—H8 | 120.3 | C11—C10—C9 | 120.1 (4) |
| C9—C8—H8 | 120.3 | C11—C10—H10 | 120.0 |
| C16—C17—C12 | 119.2 (4) | C9—C10—H10 | 120.0 |
| C16—C17—H17 | 120.4 | O1—C5—O2 | 125.2 (4) |
| C12—C17—H17 | 120.4 | O1—C5—C4 | 124.5 (4) |
| C10—C11—C6 | 118.3 (4) | O2—C5—C4 | 110.2 (4) |
| C10—C11—H11 | 120.8 | C16—C15—C14 | 119.0 (4) |
| C6—C11—H11 | 120.8 | C16—C15—C18 | 118.9 (4) |
| C14—C13—C12 | 119.6 (4) | C14—C15—C18 | 122.2 (4) |
| C14—C13—H13 | 120.2 | C18—C19—H19A | 109.5 |
| C12—C13—H13 | 120.2 | C18—C19—H19B | 109.5 |
| C13—C14—C15 | 120.4 (4) | H19A—C19—H19B | 109.5 |
| C13—C14—H14 | 119.8 | C18—C19—H19C | 109.5 |
| C15—C14—H14 | 119.8 | H19A—C19—H19C | 109.5 |
| C17—C16—C15 | 121.2 (4) | H19B—C19—H19C | 109.5 |

| | | | |
|---|---|---|---|
| C9—N1—N2—C12 | 179.0 (4) | C16—C17—C12—N2 | −179.3 (4) |
| C1—C2—C3—C4 | 1.3 (6) | C14—C13—C12—C17 | 1.7 (7) |
| C5—O2—C6—C7 | −126.7 (4) | C14—C13—C12—N2 | 179.2 (4) |
| C5—O2—C6—C11 | 58.0 (6) | C14—C13—C12—N2 | 179.2 (4) |
| C7—C6—C11—C10 | 1.6 (7) | N1—N2—C12—C17 | −172.4 (4) |
| O2—C6—C11—C10 | 176.7 (4) | N1—N2—C12—C17 | −172.4 (4) |
| C12—C13—C14—C15 | −0.3 (7) | N1—N2—C12—C13 | 10.0 (6) |
| C12—C17—C16—C15 | 0.1 (7) | N1—N2—C12—C13 | 10.0 (6) |
| C7—C8—C9—C10 | 2.3 (7) | C6—C11—C10—C9 | −0.3 (7) |
| C7—C8—C9—N1 | −178.7 (4) | C8—C9—C10—C11 | −1.7 (7) |
| C7—C8—C9—N1 | −178.7 (4) | N1—C9—C10—C11 | 179.5 (4) |
| N2—N1—C9—C8 | 171.0 (4) | N1—C9—C10—C11 | 179.5 (4) |
| N2—N1—C9—C8 | 171.0 (4) | C6—O2—C5—O1 | 4.3 (7) |
| N2—N1—C9—C10 | −10.1 (6) | C6—O2—C5—C4 | −177.0 (4) |
| N2—N1—C9—C10 | −10.1 (6) | C3—C4—C5—O1 | 174.6 (5) |
| C11—C6—C7—C8 | −1.0 (7) | S1—C4—C5—O1 | −3.6 (6) |
| O2—C6—C7—C8 | −176.2 (4) | C3—C4—C5—O2 | −4.2 (7) |
| C9—C8—C7—C6 | −1.0 (7) | S1—C4—C5—O2 | 177.7 (3) |
| C3—C2—C1—S1 | −0.5 (5) | C17—C16—C15—C14 | 1.3 (7) |
| C3—C2—C1—Br1 | −179.5 (3) | C17—C16—C15—C18 | 179.8 (4) |
| C4—S1—C1—C2 | −0.3 (4) | C13—C14—C15—C16 | −1.2 (6) |
| C4—S1—C1—Br1 | 178.8 (3) | C13—C14—C15—C18 | −179.6 (4) |
| C2—C3—C4—C5 | −179.7 (5) | O3—C18—C15—C16 | −4.3 (7) |
| C2—C3—C4—S1 | −1.5 (5) | O3—C18—C15—C16 | −4.3 (7) |
| C1—S1—C4—C3 | 1.0 (4) | C19—C18—C15—C16 | 175.2 (4) |
| C1—S1—C4—C5 | 179.5 (4) | O3—C18—C15—C14 | 174.1 (5) |
| C16—C17—C12—C13 | −1.6 (7) | O3—C18—C15—C14 | 174.1 (5) |
| C16—C17—C12—N2 | −179.3 (4) | C19—C18—C15—C14 | −6.4 (7) |

*Hydrogen-bond geometry (Å, º)*

| *D*—H···*A* | *D*—H | H···*A* | *D*···*A* | *D*—H···*A* |
|---|---|---|---|---|
| C13—H13···N1 | 0.95 | 2.47 | 2.722 (6) | 95 |
| C16—H16···O3 | 0.95 | 2.49 | 2.788 (6) | 98 |
| C10—H10···N2 | 0.95 | 2.45 | 2.705 (6) | 95 |